LAUNCHER AERODYNAMIC ANALYSIS WITH PLUME EFFECTS

Antonio Viviani* and Giuseppe Pezzella**
***Department of Engineering. University of Campania "L. Vanvitelli".**
****Analysis and Extrapolation to Flight Laboratory. Italian Aerospace Research Centre.**

Keywords: *Aerodynamics, Computational Fluid Dynamics, Expendable launcher, Plume effects.*

Abstract

This paper deals with the Computational Fluid Dynamics results of design analyses carried out for an expendable launcher.

The primary aim of this research effort is the flowfield simulation of the vehicle during ascent with and without rocket plume in order to address this effect in the preliminary (i.e., phase-A level) aerodynamic database of the launcher.

In this framework, full three-dimensional computational fluid dynamics analyses have been extensively performed in the range between Mach 0.5 and 5. The rocket plume is accounted in the CFD simulation by means of proper boundary condition at launcher/booster base.

1 Introduction

High reliable performance launcher demands for accurate aerodynamic analysis to address pressure and skin friction loads the vehicle has to withstand during ascent [1, 2].

In this framework, present paper deals with the Computational Fluid Dynamics (CFD) results of design analyses carried out for a typical expendable launcher configuration made of a central hammerhead fuse with two strap-on boosters.

In particular, the primary aim of this research effort is the flowfield simulation of the vehicle during ascent with and without rocket plume in order to address this effect in the preliminary (i.e., phase-A level) aerodynamic database of the launcher [3].

Full three-dimensional CFD analyses have been extensively performed in the range between Mach 0.5 and 5.

The rocket plume is accounted in the CFD simulation by means of proper boundary condition at launcher/booster base [3, 5].

Finally, note that numerical flowfield analysis are performed with Fluent code and perfect gas flow model with 7 degrees of freedom (dof) to account for air's molecules vibration at hypersonic speeds.

2 Launcher Vehicle

The launcher vehicle is shown in Fig. 1. As shown, it features a hummer head cylinder, as main body, with two strap-on boosters. The aeroshape under investigation also features a central core stage with a remarkable boat-tail configuration, which ends in correspondence of booster stage [6-10]. Non-dimensional aeroshape sizes are also reported in figure, being L the launcher height.

The fairing diameter is 16% launcher height, while that of booster is equal to 0.076 L. The booster length is forty percent of whole launcher's height.

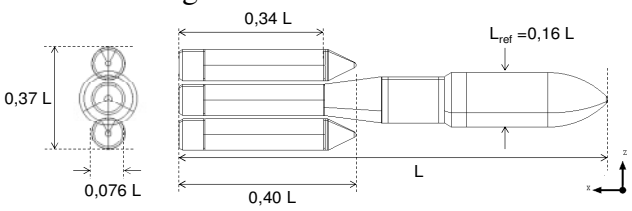

Fig. 1. The Launcher configuration.

3 Numerical Analysis

Steady-state flowfield analyses are extensively performed ranging Mach number (M_∞) from 0.5 to 5 and angle of attack (AoA) from 0 to 7 deg, according to the CFD test matrix in Tab.1.

In particular, six Mach numbers, namely 0.5, 0.9, 1.1, 1.6, 2.5, and 5 are investigated at three AoAs, namely 0, 5, and 7 deg [11].

	Mach					
AoA, deg	**0.5**	**0.9**	**1.1**	**1.6**	**2.5**	**5**
0	E	E, E-MO	E	E	E	E, E-MO
5	E	E, E-MO	E	E	E, NS	NS, NS-MO
7	E	E	E	E	E	E, E-MO

E: Eulerian CFD Motor-Off
NS: Navier-Stokes CFD Motor-Off
E-MO: Eulerian CFD Motor-On
NS: Navier-Stokes CFD Motor-On

Tab. 1. The CFD test matrix.

As one can see, fluid dynamics investigations are carried out by means of both Euler (E) and Navier-Stokes (NS) computations.

An overview of the mesh domain for both subsonic and sup-hypersonic speed flow is shown in Fig. 2 [12].

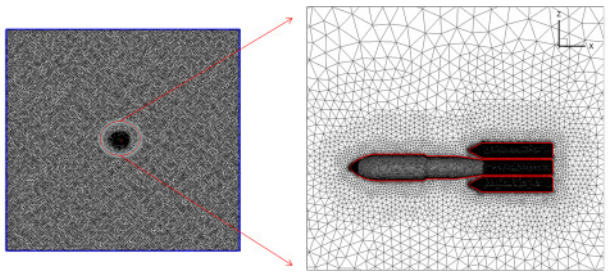

(a) Subsonic grid

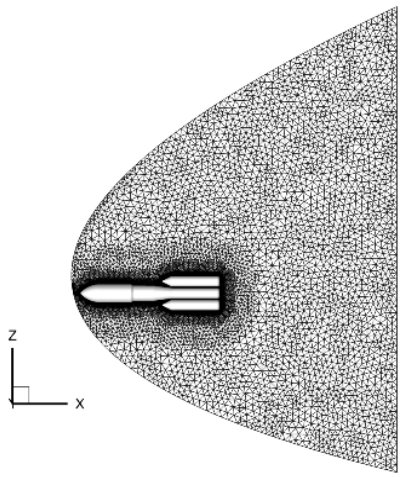

(b) Super-Hypersonic grid

Fig. 2. Overview of the hybrid mesh domain for both subsonic and sup-hypersonic speed.

Perfect gas flow model is considered for the air and rocket exhaust plume; while seven dof are activated in the computations to account for air's molecules vibration at hypersonic speeds.

In particular, all CFD simulations are performed with Fluent© code on several unstructured hybrid meshes and for both motor-off and motor-on (MO) conditions (so far, only for M=0.9 and M=5, see Tab.1).

Nozzle exit conditions considered in the computations depend on the investigated ascent flight point and are close to about T_e=2300 K, P_e=47 KPa, and M_e=3 in the hypersonic phase.

The SST k-ω turbulence flow model and cold wall boundary condition (i.e., T_w=300 K) are considered in the NS computations.

Finally, note that in the present research effort, launcher aerodynamics for both motor-off and motor-on conditions is presented and discussed.

3.1 Flowfield Results

The flow regime investigated for the launcher aerodynamic appraisal encompasses subsonic, transonic-supersonic and hypersonic regimes [13-15]. As an example of CFD results, Fig. 3 shows the surface contours of pressure and the iso-Mach surface (M=3) that takes place in the flowfield past the launcher flying at Mach 5 and 0 deg AoA.

As shown, the shape of the rocket plume is also clearly recognizable together with flow streamtraces at those flight conditions.

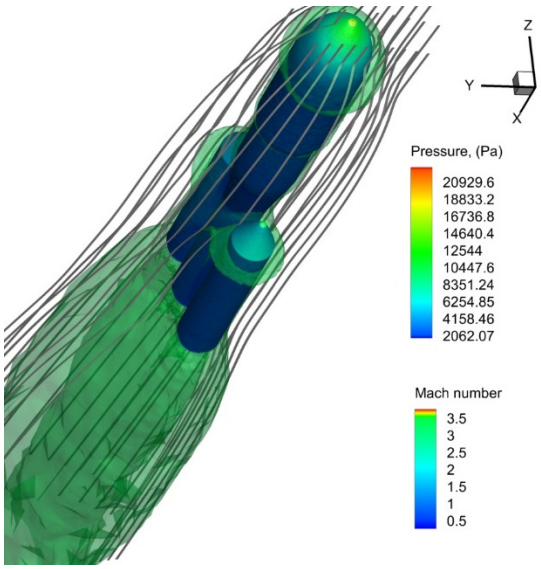

Fig. 3. Plume shape at M_∞=5 and α=0 deg.

Contours of static temperature distribution over the surface and the symmetry plane of the

launch vehicle when it is flying at M_∞=5 and α=0 deg are provided in Fig. 4.

As one sees, flow streamlines in the rocket plume are also provided, thus better appreciating the rocket plume behind the launcher.

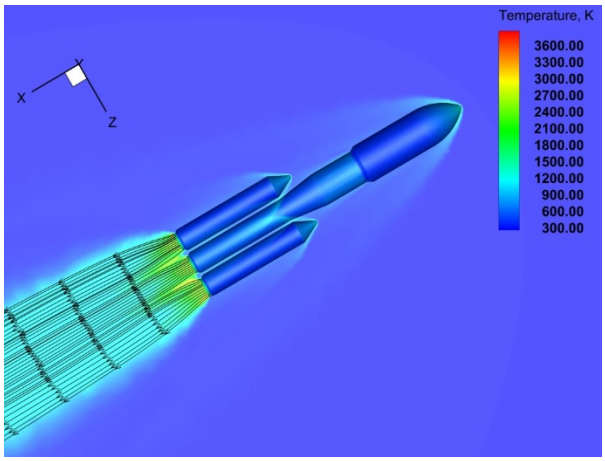

Fig. 4. Temperature flowfield contours at M_∞=5 and α=0 deg, with rocker plume streamtraces.

Further, the comparison between Mach number fields about the launcher at M_∞=5 and α=0 deg with and without rocket plume is provided in Fig. 5. As a result, this figure points out that plume effects on launcher aerodynamics could be expected.

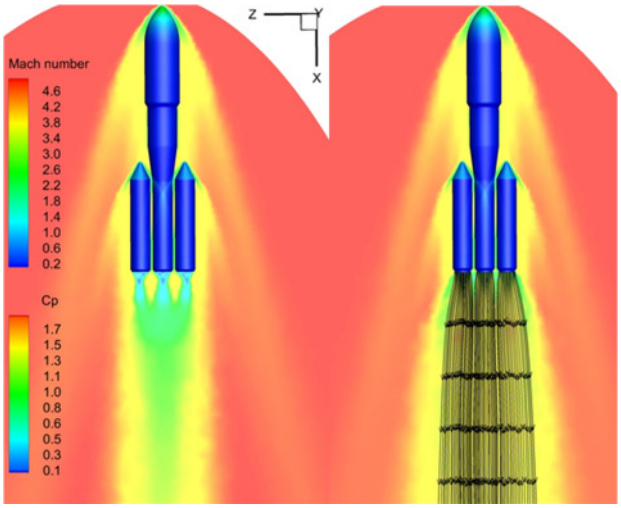

Fig. 5. Mach number contours field at M_∞=5 and α=0 deg with pressure distribution on the launcher surface. Comparison between Motor-off (left) and Motor-on conditions.

Above flowfield results are summarized in the aerodynamic performance and results comparison between motor-off and motor-on conditions provided in the next paragraph 3.2.

3.2 Aerodynamic Results

Aerodynamic data for launchers are provided in both the body reference frame (BRF), illustrated in Fig. 6, and wind reference frame (WRF).

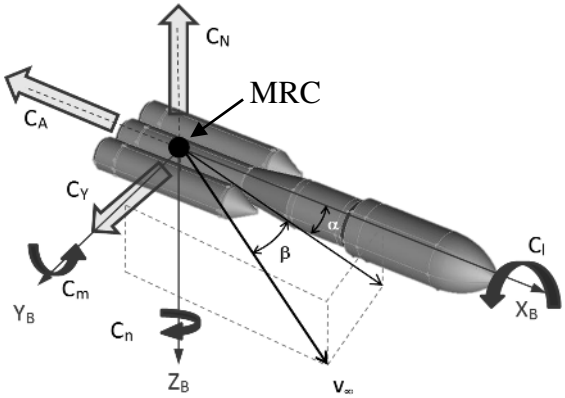

Fig. 6. The body reference frame according to the ISO 1151

In this figure, aerodynamic body force and moment coefficients, i.e., C_A, C_N, Cm, provided in the paper are also provided, with sign convention according to the ISO norm. 1151.

Lift and drag coefficients (i.e., force and moment coefficients in WRF) C_L and C_D are also presented.

Note that, the reference quantities (see Fig. 1) are:

$$L_{ref}=0.16L \qquad (1)$$

$$S_{ref}=\frac{\pi L_{ref}^2}{4} \qquad (2)$$

The aerodynamic pitching moment, Cm, is provided at the launcher nose. Usually, a conventional location, namely moment reference centre (MRC), see Fig. 6 is chosen.

Anyway, recall that the relationship for the pitching moment coefficient evaluation, passing from MRC to CoG, reads:

$$(C_m)_{CoG}=(C_m)_{MRC}+C_N\frac{\Delta x}{L_{ref}}-C_A\frac{\Delta z}{L_{ref}} \qquad (3)$$

where

$$\Delta x = x_{CoG} - x_{MRC} \quad (4)$$

and

$$\Delta z = z_{CoG} - z_{MRC} \quad (5)$$

are evaluated in the Layout Reference Frame (LRF), as shown in Fig. 7.

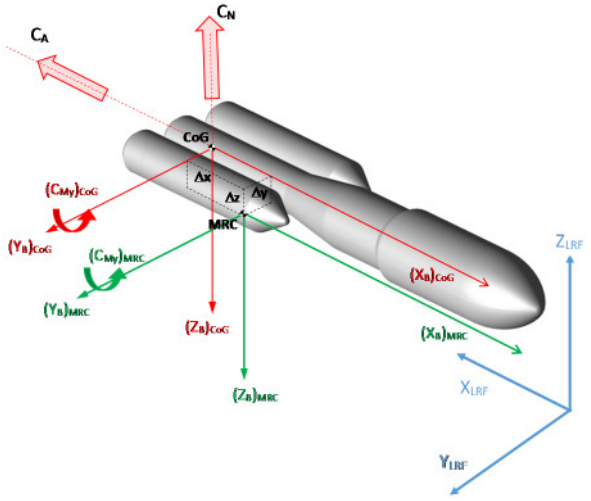

Fig. 7. The Layout reference frame (LRF).

As far as aerodynamic coefficients are concerned, launcher drag force, lift force and pitching moment coefficients are summarized from Fig. 8 to Fig. 17.

Note that, aerodynamic coefficients are important at system level for the assessment of launcher general loading determinations, performances and, as well as, guidance, navigation and attitude control. For instance, performances studies use the axial force coefficient C_A since this aerodynamic force opposes to the vehicle movement. Indeed, the axial force coefficient versus Mach at 0 deg AoA is shown in Fig. 8.

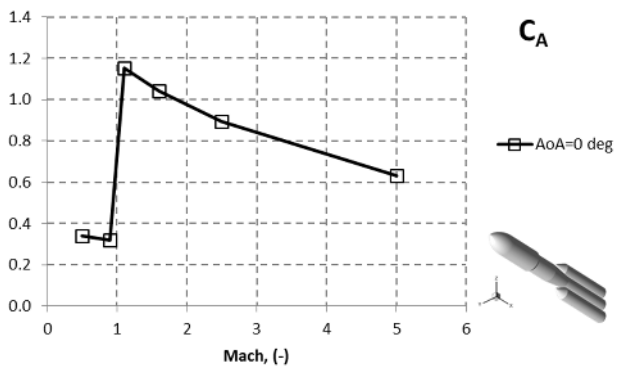

Fig. 8. Axial coefficient versus M_∞ at α=0 deg.

The effect of flow compressibility is remarkable, as expected. Indeed, the strong increase to which undergoes the axial aerodynamic force, when M_∞ becomes transonic, is due to the wave drag contribution, as expected.

Nevertheless, this contribution tends to be less strong as Mach number goes towards hypersonic speed conditions considering that the shock becomes weak due to the streamlined vehicle aeroshape (i.e., high inclined shock to assure a narrow shock layer).

Launcher drag, lift and pitching moment coefficients at M_∞=0.5 and for α ranging from -10 to 10 deg are shown form Fig. 9 to Fig. 11.

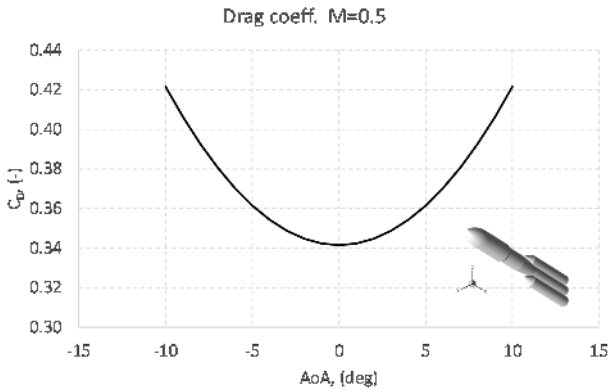

Fig. 9. Drag coefficient versus alpha at M_∞=0.5.

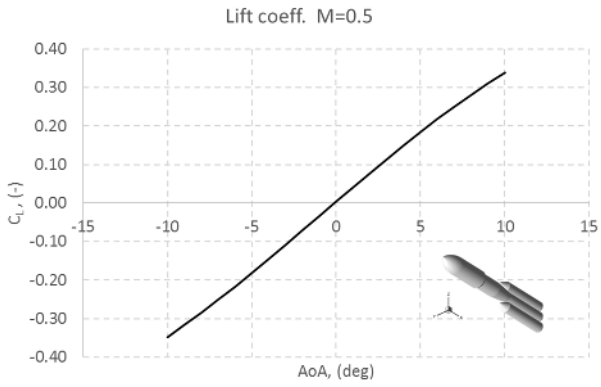

Fig. 10. Lift coefficient versus alpha at M_∞=0.5.

As shown, lift, drag and pitching moment coefficients feature a non-linear behaviour versus alpha, with C_D that exhibits the classical parabolic evolution at all flight conditions under investigation.

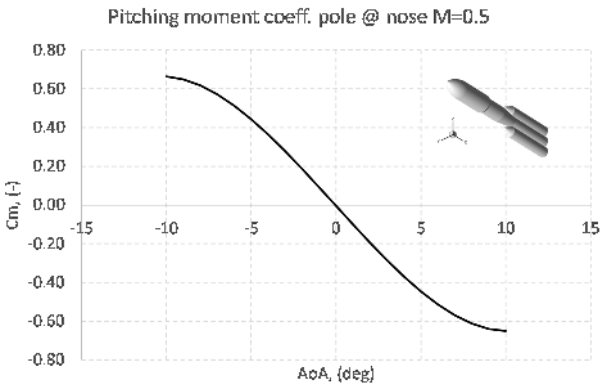

Fig. 11. Pitching moment coefficient versus alpha at M_∞=0.5. Pole at launcher nose.

The same aerodynamic characteristics are also reported for both M_∞=1.1 and 5.0 form Fig. 12 to Fig. 17.

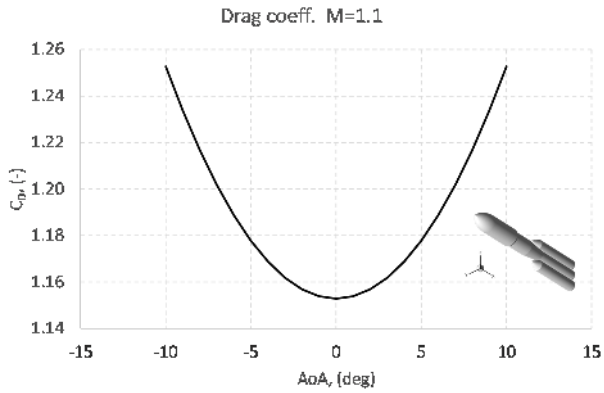

Fig. 12. Drag coefficient versus alpha at M_∞=1.1.

Fig. 13. Lift coefficient versus alpha at M_∞=1.1.

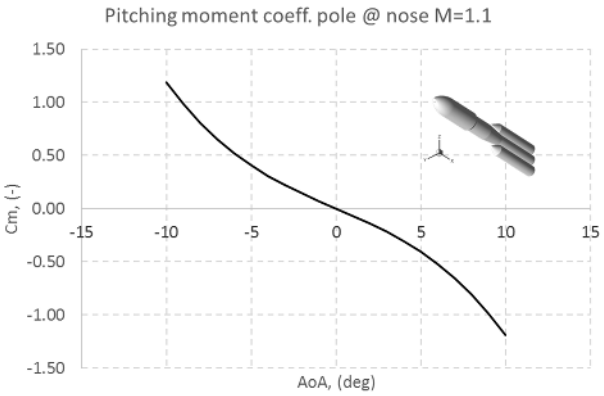

Fig. 14. Pitching moment coefficient versus alpha at M_∞=1.1. Pole at launcher nose.

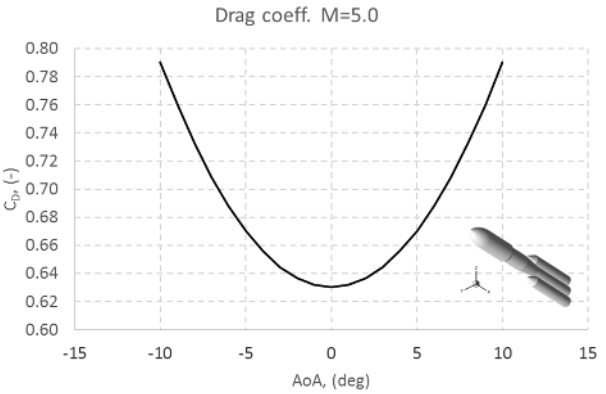

Fig. 15. Drag coefficient versus alpha at M_∞=5.0.

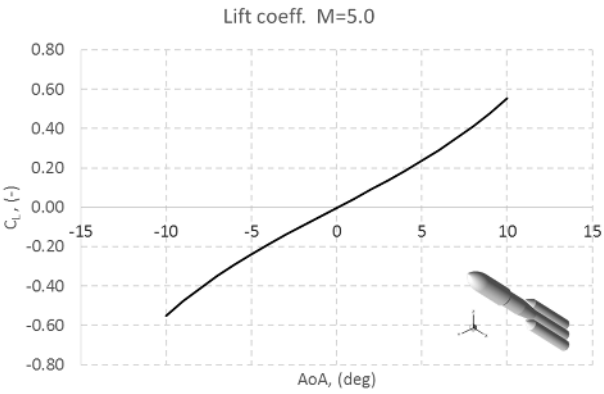

Fig. 16. Lift coefficient versus alpha at M_∞=5.0.

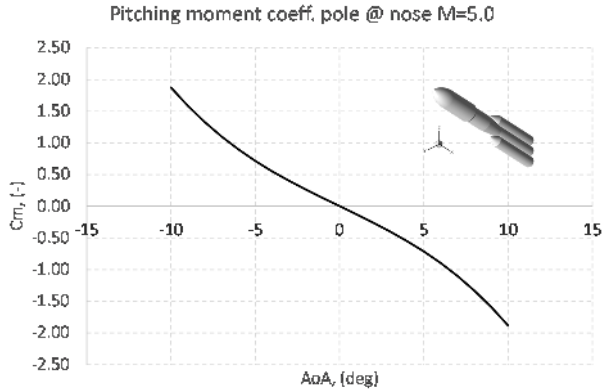

Fig. 17. Pitching moment coefficient versus alpha at M_∞=5.0. Pole at launcher nose.

Note that both C_L and Cm at α=0 deg are null due to the symmetric launcher aeroshape.

As far as rocket plume effects on aerodynamics are concerned, in Table 2 and Table 3 aerodynamic coefficients for both motor-on and motor-off conditions are provided at M_∞=0.9 and 5.0, respectively. In table 2 results refers to only two AoAs, namely 0 and 5 deg; while for M=5.0 all the angles of attack, i.e. 0, 5, and 7 deg are reported.

M=0.9 @ Motor-ON					
AoA	CA	CN	CM	CD	CL
0	0.25010	-0.00076	0.00924	0.25010	-0.00076
5	0.25077	0.10215	-0.12492	0.25872	0.07991

M=0.9 @ Motor-OFF					
AoA	CA	CN	CM	CD	CL
0	0.32551	0.00497	-0.03133	0.32551	0.00497
5	0.33174	0.11816	-0.23929	0.34077	0.08879

Tab. 2. Aerodynamic coefficients for motor-on and motor-off conditions at M_∞=0.9.

M=5.0 @ Motor-ON					
AoA	CA	CN	CM	CD	CL
0	0.63372	0.00016	0.00293	0.63372	0.00016
5	0.65251	0.31781	-0.81496	0.67773	0.25973
7	0.66378	0.43506	-1.10507	0.71186	0.35092

M=5.0 @ Motor-OFF					
AoA	CA	CN	CM	CD	CL
0	0.63045	-0.00093	0.00414	0.63045	-0.00093
5	0.64758	0.29590	-0.71644	0.67091	0.23833
7	0.66204	0.43479	-1.10581	0.71009	0.35086

Tab. 3. Aerodynamic coefficients for motor-on and motor-off conditions at M_∞=5.

As one can see, present phase-A aerodynamic analysis points out that there are no differences between launcher aerodynamic coefficients passing from motor-off to motor-on conditions at hypersonic flow conditions.

On the contrary, at M=0.9 flight conditions significant differences can be appreciated, as summarized in the following Table 4.

	Percentage reduction due to Rocket Plume effects				
AoA	ΔCA	ΔCN	ΔCM	ΔCD	ΔCL
0	23.2	115.2	129.5	23.2	115.2
5	24.4	13.5	47.8	24.1	10.0

Tab. 4. Percentage differences between aerodynamic coefficients for motor-on and motor-off conditions at M_∞=0.9.

Indeed, at motor-on conditions a reduction of about 24%, 10%, and 50% is fund for drag, lift and pitching moment coefficients, respectively.

In particular, the rocket plume results in a pitch-up effect for the launcher.

4 Conclusions

In this research effort launcher aerodynamic design activities at phase-A level are described.

The goal is to address the preliminary aerodynamic database of a next generation launch vehicle as input for performances evaluations as well as launcher control, sizing, and staging dynamics. To this end, steady state computational fluid dynamics, with both Euler and Navier-Stokes approximations, are carried out at six Mach numbers, namely 0.5, 0.9, 1.1, 1.6, 2.5, and 5, and at three angle of attacks, i.e., α=0, 5, and 7 deg,. For this test matrix, launcher aerodynamic performance in terms of axial, normal, drag, lift and pitching moment coefficients is provided. Numerical results point out that the axial force coefficient does not significantly change passing from 0 to 7 deg angle of attack at each considered Mach number; while the effect of flow compressibility is remarkable.

Regarding lift, drag and pitching moment coefficients, results highlight that, for each Mach number, it features a quite non-linear slope as the angle of attack increases up to 10 deg.

Finally, the launcher aerodynamic coefficients investigated at Mach 5 point out that no difference are expected passing from motor-off to motor-on conditions.

On the contrary, at M=0.9 flight conditions significant differences can be appreciated. At motor-on conditions a reduction of about 24%, 10%, and 50% is fund for drag, lift and pitching moment coefficients, respectively.

In particular, the rocket plume results in a pitch-up effect for the launcher.

References

[1] Klopfer, G. H., Klessy, J. E., Leez, H. C., Onuferx, J. T., Pandy, S., and Chank, W. M., "Validation of Overflow for Computing Plume Effects during the Ares I Stage Separation Process". 49th AIAA Aerospace Sciences Meeting including the New Horizons Forum and Aerospace Exposition 4 - 7 January 2011, Orlando, Florida. AIAA 2011-170.

[2] Gusman, M., Housman, J., Kiris C., "Best Practices for CFD Simulations of Launch Vehicle Ascent with Plumes - OVERFLOW Perspective". 49th AIAA Aerospace Sciences Meeting, Jan. 4–7, 2011, Orlando, Fl.

[3] Viviani, A., Pezzella, G., "Computational Flowfield Analysis of a Next Generation Launcher". 6th European Conference for Aeronautics and Space Sciences (Eucass). 29 June- 3 July. 2015 Krakow. Poland.

[4] Viviani, A., Pezzella, G., "Next Generation Launchers Aerodynamics". Research Signpost, T.C. 37/661 (2), Fort P.O., Trivandrum-695 023. Kerala, India. ISBN: 978-81-308-0512-2

[5] Viviani, A., Pezzella, G., "Numerical Analysis of the Flowfield Past a Next Generation Launcher". 20th AIAA Hypersonics. Strathclyde University Technology & Innovation Center. 6-9 July 2015 Glasgow. Scotland. AIAA-2015-3535. doi: 10.2514/6.2015-3644.

[6] Viviani, A., Pezzella, G., D'Amato, E., "Aerodynamic Analysis with Separation Dynamics of a Launcher at Staging Conditions". 30th Congress of International Council of the Aeronautical Sciences. ICAS 2016. DDC Daejeon Korea. September 25-30, 2016.

[7] Rogers, S. E., Dalle, D. J., and Chan, W. M., "CFD Simulations of the Space Launch System Ascent Aerodynamics and Booster Separation", 53rd AIAA Aerospace Sciences Meeting, AIAA SciTech Forum, (AIAA 2015-0778) https://doi.org/10.2514/6.2015-077.

[8] Pezzella, G., "Aerodynamic and Aerothermodynamic design of Future Launchers Preparatory Program Concepts". Aerospace Science and Technology, Volume 23, Issue 1, December 2012, Pages 233–249. http://dx.doi.org/10.1016/j.ast.2011.07.011.

[9] Pezzella, G., Viviani, A., "Launcher Aerodynamics: a Suitable Investigation Approach at Phase-A Design Level". Book title: Advances in Hypersonic Vehicles Technologies. Published by In-Tech. Kirchengasse 43/3, A-1070 Vienna, Austria. Hosti 80b, 51000 Rijeka, Croatia. DOI: 10.5772/intechopen.68209. ISBN: 978-953-51-3904-1. Print ISBN: 978-953-51-3903-4.

[10] Pezzella, G., Marini, M., Roncioni, P., Kauffmann, J., Tomatis, C., "Preliminary Design of Vertical Takeoff Hopper Concept of Future Launchers Preparatory Program", Journal of Spacecraft and Rockets 2009. ISSN 0022-4650 vol.46 no.4 (788-799) doi: 10.2514/1.39193

[11] Bertin, J., J., "Hypersonic Aerothermodynamics". AIAA Education Series. 1994. Washington

[12] Anderson, J. D., "Hypersonic and High Temperature Gas Dynamics", McGraw-Hill Book Company, New York, 1989.

[13] F. Petrosino, M. De Stefano Fumo, G. Pezzella, "Evolution of Aerodynamic Shape for a Concept of Autonomous Re-Entry Vehicle", 31st AIAA Applied Aerodynamics Conference. 24 - 27 June 2013. San Diego, California. doi: 10.2514/6.2013-2664.

[14] F. Petrosino, D. Cinquegrana, G. Andreutti, F. Capizzano, P. Catalano, G. Pezzella, M. De Stefano Fumo, "Aerodynamic Analysis of the USV3 Vehicle from Hypersonic to Landing Flight Conditions", 64rd International Astronautical Congress. IAC-2013. 23-27 Sept, 2013. Beijing, China. IAC-13-D2.3.

[15] D. Cinquegrana, R. Gardi, V. De Simone, F. Petrosino, P. Catalano, G. Pezzella, M. De Stefano Fumo, "Aerothermodynamic and TPS Design Analysis of the USV3 Re-Entry Vehicle", 64rd International Astronautical Congress. IAC-2013. 23-27 Sept, 2013. Beijing, China. IAC-13-D2.3.1.19286.

5 Contact Author Email Address

The contact author email addresses are: antonio.viviani@unicampania.it g.pezzella@cira.it.

Copyright Statement